Radial Single-Shot STEAM MRI

Kai Tobias Block* and Jens Frahm

Rapid MR imaging using the stimulated echo acquisition mode (STEAM) technique yields single-shot images without any sensitivity to resonance offset effects. However, the absence of susceptibility-induced signal voids or geometric distortions is at the expense of a somewhat lower signal-to-noise ratio than EPI. As a consequence, the achievable spatial resolution is limited when using conventional Fourier encoding. To overcome the problem, this study combined single-shot STEAM MRI with radial encoding. This approach exploits the efficient undersampling properties of radial trajectories with use of a previously developed iterative image reconstruction method that compensates for the incomplete data by incorporating a priori knowledge. Experimental results for a phantom and human brain in vivo demonstrate that radial single-shot STEAM MRI may exceed the resolution obtainable by a comparable Cartesian acquisition by a factor of four. Magn Reson Med 59:686–691, 2008. © 2008 Wiley-Liss, Inc.

Key words: turboSTEAM; stimulated echoes; rapid imaging; iterative reconstruction; compressed sensing

Single-shot STEAM MRI is a rapid imaging technique based on a train of stimulated echoes that are generated by low-flip angle readout RF pulses from a pool of longitudinal magnetization prepared by two preceding 90° RF pulses (1). Its major advantage is that all echoes are RF refocused, making the sequence insensitive to artifacts from off-resonance effects. Therefore, single-shot STEAM MRI can be used to acquire distortion-free images from brain areas with severe tissue susceptibility differences that are often hardly accessible using gradient-echo sequences such as echo planar imaging (EPI). Further advantageous characteristics are the much lower RF power deposition in comparison to single-shot fast spin-echo sequences, in particular at higher magnetic field strengths, and the decay of the stimulated echo intensities with the T1 relaxation time which under in vivo conditions is usually much longer than the T2 relaxation time.

A major limitation of the STEAM technique is that half of the magnetization is unavoidably lost during the preparation of the pre-encoded longitudinal magnetization. As a consequence, the resulting images have a lower signal-to-noise ratio (SNR) than, for example, echo-planar images. Moreover, for a typical T1 relaxation time, receiver bandwidth, and low-flip angle RF pulses, the echo train length is limited to about 50 usable stimulated echoes. This value certainly restricts the spatial resolution for conventional Fourier encoding even when combining a rectangular FOV with partial Fourier encoding or parallel imaging. In practice, optimized applications to the human brain yield 2 mm isotropic resolution as already demonstrated for diffusion-weighted single-shot STEAM MRI (2,3).

The purpose of this work was to adopt radial encoding strategies for single-shot STEAM MRI. Radial trajectories provide unique properties including a low sensitivity to object motion, as earlier demonstrated for conventional single-echo STEAM MRI (4), and effective undersampling abilities. Recently, we presented an iterative algorithm for the reconstruction from undersampled radial acquisitions, which allows to reduce the amount of sampled data to a degree currently not achievable using Fourier encoding (5). Proof-of-principle applications dealt with radial spin-echo MRI of the human brain. However, when using gradient-echo sequences, the advantages of radial trajectories are compromised by a high sensitivity to off-resonance effects that lead to serious complications for a multi-echo scenario. In contrast, this sensitivity is not an issue when using radial encodings for single-shot STEAM MRI: while stimulated echoes eliminate the off-resonance sensitivity of the radial trajectory, the undersampling abilities of radial encoding allow to overcome the resolution limitations of Cartesian single-shot STEAM MRI.

THEORY

Sequence Design

Figure 1 shows a timing diagram of a generic single-shot STEAM MRI sequence with radial encoding. The sequence starts with a spoiler gradient (a) to ensure complete dephasing of any residual transverse magnetization components from preceding measurements. Slice-selective excitation is accomplished using a first 90° pulse (b) in the presence of gradient (*c*). Proper refocusing of this gradient involves the gradient (*e*), the corresponding slice-selective gradients (*g*) and (*j*) for the second 90° pulse (f) and the low-flip angle read pulse (i), and the spoiler gradient (*m*) which is required for dephasing of the unwanted free induction decay elicited by pulse (i). During the first TE/2 interval, the dephasing of all transverse magnetizations, which is the stimulated echo condition (6), is accomplished by gradient (*d*) along the read direction. Any transverse magnetization during the first TM interval is effectively removed by a spoiler gradient (*h*) in the read direction.

The acquisition part of the single-shot STEAM MRI sequence encompasses multiple repetitions of the final TE/2 interval with different orientations for the effective readout gradient (*n*, *o*). The starting point of a particular spoke in *k*-space is reached by the dephasing gradients (*k*) and (*l*) in read and phase direction, respectively. After data acquisition, the transverse magnetization components are returned to the center of *k*-space by rewinder gradients in read (*p*) and phase (*q*) direction.

The waveforms of all varying gradients (dotted lines in Fig. 1) can be calculated once for the maximum moment needed and then played out with scaled amplitudes. This

Biomedizinische NMR Forschungs GmbH am Max-Planck-Institut für Biophysikalische Chemie, Göttingen, Germany

*Correspondence to: T. Block, Biomedizinische NMR Forschungs GmbH, 37070 Göttingen, Germany. E-mail: tblock@gwdg.de

Received 4 April 2007; revised 3 July 2007; accepted 2 August 2007.

DOI 10.1002/mrm.21401

Published online in Wiley InterScience (www.interscience.wiley.com).

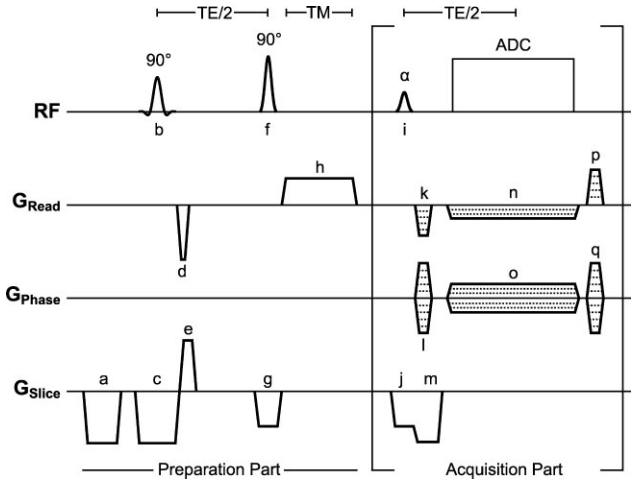

FIG. 1. Schematic diagram for radial single-shot STEAM MRI. For details see text.

ensures a fixed sequence timing for all repetitions. The amplitude of the readout gradients for a spoke with angle ϕ is simply given by $A_{\text{read}} = A_{\max} \cdot \sin\phi$ and $A_{\text{phase}} = A_{\max} \cdot \cos\phi$, where $A_{\max}$ denotes the amplitude of the maximum moment gradient. To take full advantage of the initially prepared longitudinal magnetization and at the same time allow for a more homogeneous signal intensity for all stimulated echoes, variable flip angles were applied as described previously (3).

Ordering Schemes

Because all spokes of a radial encoding scheme are physically equivalent, the order at which specific spokes are acquired may follow different strategies. The simplest scheme would be to sample all spokes clockwise from zero to 180° as depicted in the top left of Figure 2. However, due to T1 relaxation and deviations of the generated flip angles, this scheme will lead to a sharp edge in *k*-space between the first and last spoke. Simulations of a circular phantom demonstrate that this problem causes smearing artifacts in the reconstructed image as shown in the bottom left of Figure 2. It is therefore beneficial to arrange "early" and "late" spokes acquired along the stimulated echo train more uniformly in *k*-space. A scheme which totally avoids any intensity edges is shown in the top middle of Figure 2. Despite its smooth intensity transition in the angular direction, however, this scheme leads to an unfavorable point-spread function and therefore causes object deformations in areas with a strong signal decay (bottom middle of Fig. 2). In practice, the most preferential ordering emerged as an interleaved serial scheme depicted in the upper right of Figure 2. Here, the *k*-space is sampled clockwise for several times, but each time with a different angular offset. The interleaved scheme leads to a number of edges in *k*-space, but with clearly reduced strength compared to a single clockwise sampling. Therefore, areas with a pronounced T1 signal attenuation lead to only mild smearing artifacts without object deformations. In addition, this last scheme has the interesting property that it allows for the reconstruction of separate images from each interleave. For example, if 64 spokes are sampled in a total of 8 interleaves, it is possible to reconstruct 8 images with different degrees of mean T1 attenuation along the train of stimulated echoes. Although such low-resolution images may be exploited to gain information about local T1 relaxation effects, it remains to be seen in practice whether the reduced quality will be sufficient for the estimation of adequate T1 maps.

A further variation of the ordering scheme can be achieved by reversing the direction of every second spoke in *k*-space. Instead of monotonously scanning 180° of *k*-space as shown in the upper left of Figure 3, this scheme leads to angles ranging from zero to 360° (top right of Fig. 3). The lower row shows corresponding image reconstructions from simulated data of an off-resonant circle. As a direct consequence of the Fourier-shift theorem, unidirectional coverage of 180° of *k*-space leads to an unsymmetrical U-shaped artifact that spreads over the entire image (lower left of Fig. 3). A much more tolerable and focused artifact is obtained for the case of reversed spokes and 360° coverage (lower right of Fig. 3).

Image Reconstruction

When using conventional image reconstruction methods for radial encodings like regridding or projection reconstruction, a low number of sampled spokes causes streaking artifacts as a consequence of the unmeasured gaps in *k*-space. Further, the weighting of the raw data with the Ram–Lak filter to compensate for the varying sample density leads to a well-known amplification of image noise. Therefore, the present work utilizes a recently developed iterative approach which compensates for the undersampled information by introducing a priori knowledge about the object (5). Briefly, the approach is based on a nonlinear optimization of the inverse problem with additional penalty functions. The penalty functions are used to rate the plausibility of an image estimate and, thus, drive the algorithm to find a solution that complies with the known information about the object out of all image

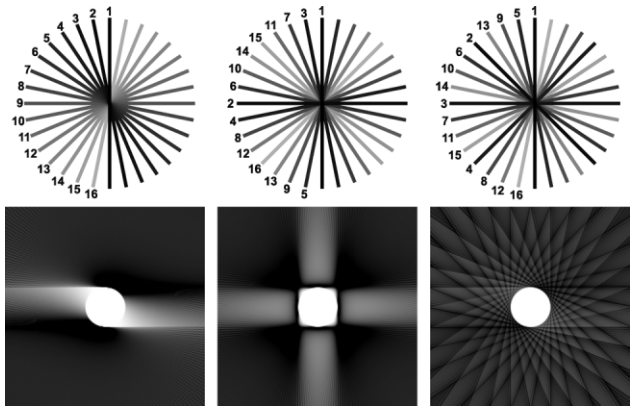

FIG. 2. (Top) Different schemes for the temporal ordering of acquired spokes in radial single-shot STEAM MRI (numbers indicate the time of sampling). (Bottom) Simulation of image artifacts caused by relaxation effects.

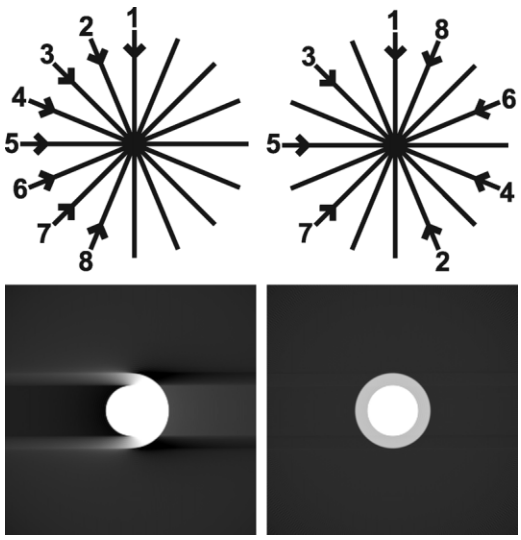

FIG. 3. Radial sampling schemes with (top left) constant and (top right) alternate spoke directions reversing every second spoke (numbers indicate the time of sampling). (Bottom) Simulation of corresponding image artifacts caused by off-resonance effects.

estimates matching the incomplete measured data. The algorithm uses prior knowledge about the extent of the object, assumes that the true object is piecewise constant, and exploits the fact that the physical quantity measured by MRI cannot take negative values.

In a setup with multiple phased-array coils, the reconstruction method first estimates the coil profiles which are then used to calculate a final real-valued image estimate constrained to positive values. Hence, the algorithm can also be seen as an auto-calibrating approach for non-Cartesian parallel imaging. As the object is assumed to be piecewise constant, a penalty on the total variation (TV) of the object is applied in the final image estimation step. The TV constraint leads to a suppression of undersampling artifacts as well as an edge-preserving denoising of the image. The degree of denoising can be selected by varying the weight for TV minimization during reconstruction of the final image.

Despite the use of variable flip angles for the readout pulses, the signal strength of the stimulated echoes decreases during acquisition. While Cartesian Fourier encoding translates this attenuation into blurring along the phase-encoding direction of the image, radial encodings suffer from smearing artifacts in the radial direction. However, because the zeroth moment of the object's projection profile should be independent of the projection angle, an approximation of the signal decay can be estimated from the spokes and used for a first-order correction. Therefore, a projection profile is calculated from the raw data of every spoke using the Fourier-slice theorem prior to the actual reconstruction. The sum of each profile is then calculated to approximate the signal intensity of the corresponding spokes. This information is later used in the iterations to weight the spokes calculated from an image estimate before comparing them to the measured data. It is important to point out that this compensation mechanism assumes a homogeneous relaxation time of the object. As the T1 relaxation time is a locally varying quantity, it will obviously fail if strong deviations are present within a particular section. However, the approach turned out to be quite effective in practice and has the advantage of being self calibrating.

MATERIALS AND METHODS

All measurements were conducted at 2.9 T (Siemens Magnetom TIM Trio, Erlangen, Germany) using a receive-only 12-channel head coil in triple mode yielding 12 channels with different combinations of the coils. A total of four subjects participated in the study. Written informed consent was obtained in all cases prior to each examination.

Radial images were acquired with a base resolution ranging from 104 to 208 pixels and a FOV of 208 mm which leads to a nominal in-plane resolution of 1–2 mm. The number of spokes varied from 32 to 80 and the receiver bandwidth from 120 to 480 Hz/pixel. Except for Figure 7, the section thickness was 4 mm and a preceding CHESS pulse was applied for fat suppression. The stimulated echo time TE and the duration of the acquisition interval TR were set to the minimum possible value in all cases. Typically, for 48 spokes, a 208 pixel base resolution, and a bandwidth of 160 Hz/pixel, the sequence resulted in TE = 9.6 ms, TR = 9.2 ms, and an overall measuring time of 464 ms. Noteworthy, in single-shot STEAM MRI, TR may be shorter than TE as the repetitive acquisition interval—which starts with a low-flip angle readout rf pulse—covers only the second half of the echo interval required for generation of a stimulated echo. The first half of the echo interval is the time between the leading two 90° RF pulses and used only once.

All radial acquisitions were performed using an ordering scheme with 8 interleaves and 360° coverage. A compensation mechanism was employed to avoid gradient timing errors and corresponding smearing artifacts due to a misalignment of the data in *k*-space (7). Reconstructions of all radial images were performed offline using an in-house software package MRISim.

The Cartesian version of single-shot STEAM MRI used here (8) employed variable flip angles for the readout RF pulses, 5/8 partial Fourier encoding, and image reconstruction with use of a projection onto convex sets (POCS) algorithm. POCS reconstructions are more appropriate than a TV minimization to handle incomplete data in the partial Fourier case. To allow for a fair comparison the images covered a 160×256 mm^2 FOV with an 50×128 acquisition matrix (receiver bandwidth 160 Hz/pixel) to yield a 2 mm in-plane resolution (best case) at 4 mm slice thickness. Spin-echo EPI images were acquired with a sequence supplied by the MRI vendor using comparable parameters where possible (256 mm FOV, 128 pixels base resolution, 5/8 partial Fourier encoding, receiver bandwidth 1345 Hz/pixel, 4 mm section thickness, effective echo time TE = 31 ms).

RESULTS

Figure 4 compares the best image resolution obtainable with Cartesian single-shot STEAM MRI to the proposed

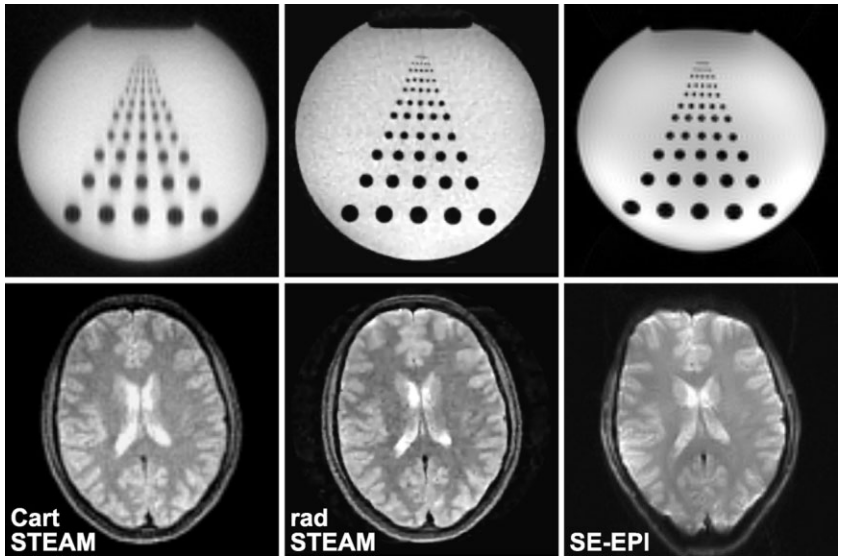

FIG. 4. Image resolution achievable using single-shot STEAM MRI with (left) Cartesian sampling and (middle) radial encoding in comparison to (right) spin-echo EPI. (Top) Water phantom (radial encoding using 48 spokes, 160 Hz/pixel bandwidth) and (bottom) transverse section of human brain in vivo (64 spokes).

radial version for cross-sectional images of a water phantom and human brain in vivo. While the Cartesian images have a 2.0 mm in-plane resolution, the radial images present with 1.0 mm resolution. This fourfold reduction in voxel size is best appreciated in the images of the water phantom, where nearly all circles are resolved by the radial method. In the brain images the improved resolution can also be clearly seen, especially when focussing on the borders of the brain or the skull. Noteworthy, the Cartesian images suffer from pronounced blurring in the phase-encoding direction, which reflects the influence of decreasing stimulated echo intensities on the respective point-spread function. For comparison, the right column of Figure 4 shows corresponding spin-echo echo-planar images. Although presenting with a better SNR, both the phantom and brain image are affected by significant distortion artifacts. These problems obviously limit the usefulness of EPI whenever reliable anatomic accurateness is required as, for example, for surgery planning using data from EPI-based diffusion tensor imaging.

The upper row of Figure 5 shows iterative image reconstructions from radial acquisitions with 48 spokes and different receiver bandwidths. Rather than affecting the SNR the increased bandwidth leads to slightly decreased image resolution and image contrast. In fact, because the TV constraint efficiently removes noise during iterative reconstruction, a lower SNR translates into a lower resolution in the final image. The somewhat lower gray-white matter contrast is caused by a shorter duration of the acquisition part (shorter TR intervals) for higher bandwidths that reduce the effective T1 weighting of the stimulated echoes. However, this is not necessarily a drawback because certain applications, including diffusion studies, do not require such image contrast. The bottom row of Figure 5 depicts reconstructions of the same data using a conventional regridding approach. Here, a higher bandwidth is accompanied by increased image noise. The images also demonstrate that a more advanced reconstruction method than regridding is required for this type of undersampled data acquisition.

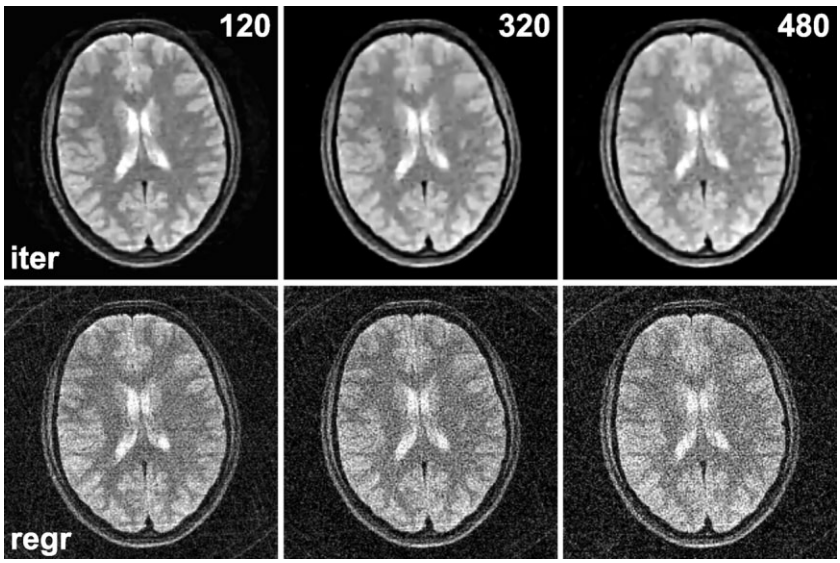

FIG. 5. (Top) Iterative and (bottom) conventional regridding reconstructions (transverse sections of the human brain in vivo) for radial single-shot STEAM MRI (48 spokes) with a bandwidth of (left) 120 Hz/pixel, (middle) 320 Hz/pixel, and (right) 480 Hz/pixel (1.0 mm nominal in-plane resolution, 4 mm section thickness).

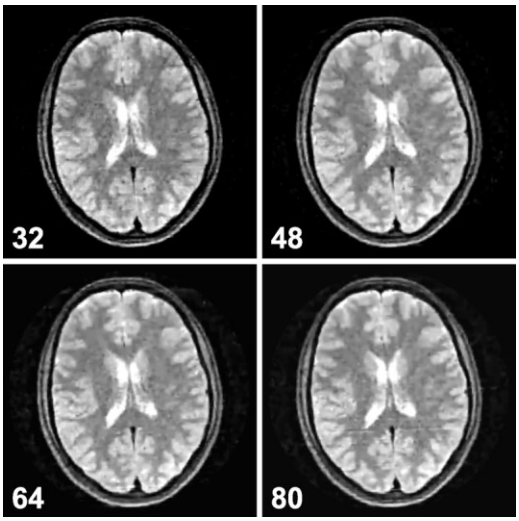

FIG. 6. Iterative reconstructions for radial single-shot STEAM MRI (transverse sections of the human brain in vivo) with 32, 48, 64, and 80 spokes (bandwidth 160 Hz/pixel, 1.0 mm nominal in-plane resolution, 4 mm section thickness).

Figure 6 shows radial images of the human brain with 32, 48, 64, and 80 spokes. Despite these differences, all iterative reconstructions recover the object with reasonable quality. The reconstruction from 32 spokes suffers from some residual undersampling artifacts leading to a lower overall resolution. In contrast, the image from 80 spokes becomes mildly affected by artificial streaks in the horizontal direction that result from localized T1 relaxation effects due to the very long echo train. In general, the images demonstrate that radial sampling offers considerable freedom for trajectory design, allowing to tailor imaging protocols for specific needs.

The range of SNR and resolution achievable by radial single-shot STEAM MRI is summarized in Figure 7 for a transverse cross-section of the human brain with a nominal in-plane resolution of 1.0–2.0 mm and a section thickness of 2.0–4.0 mm. The reduced SNR for higher in-plane resolution is due to both an increased bandwidth needed to maintain the sequence timing and a larger degree of undersampling. Similar to the findings in Figure 5, increased noise in the data acquisition is not necessarily visible in the iteratively reconstructed images because of the TV constraint. A decrease of the section thickness is accompanied by a significantly higher noise level that lowers the reconstructed image resolution. This can be best seen for the highest in-plane resolution where proper windowing would reveal additional noise patterns in the background of the object for a 2 mm section thickness.

DISCUSSION

The use of radial trajectories allows to overcome the practical resolution limit for single-shot STEAM MRI when using Cartesian Fourier encoding (spin-warp imaging). While low SNR of the acquired data remains a persistent problem, the constrained variation of the image intensity as part of the used iterative reconstruction method yields images

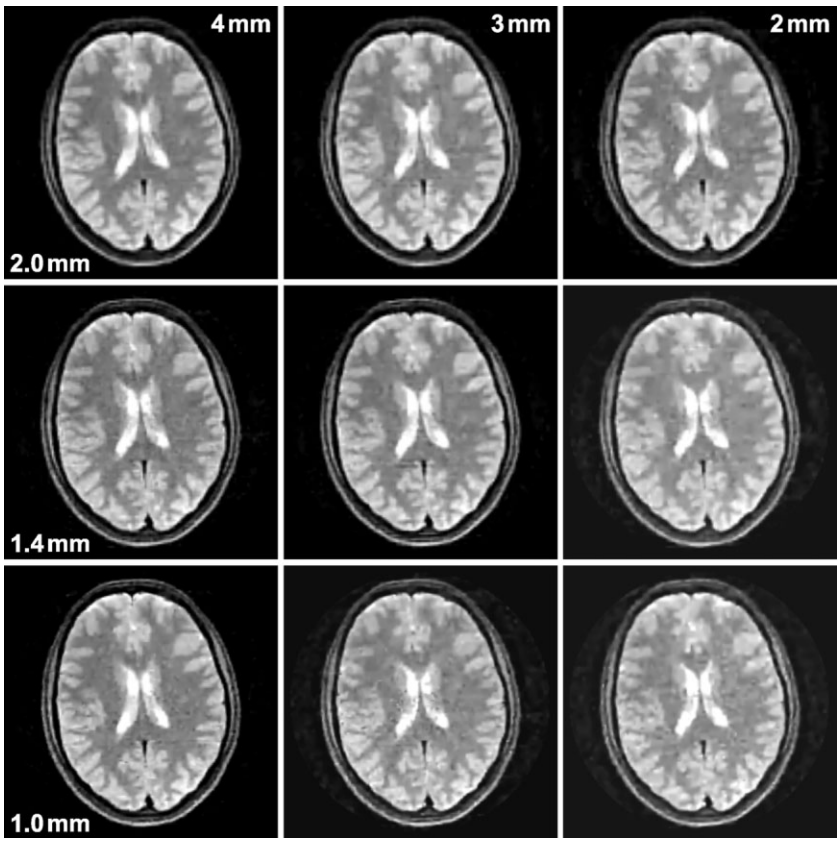

FIG. 7. Iterative reconstructions for radial single-shot STEAM MRI (transverse sections of the human brain in vivo) with a nominal in-plane resolution of (top) 2.0 mm, (center) 1.4 mm, and (bottom) 1.0 mm and a section thickness of (left) 4 mm, (middle) 3 mm, and (right) 2 mm (48 spokes, bandwidth 160 Hz/pixel).

without visible noise artifacts. In fact, TV minimization techniques are among the most powerful methods currently available for general image denoising, especially due to the preservation of sharp edges. Nevertheless, the approach is only able to remove oscillating intensity fluctuations between neighboring pixels and, hence, only flattens noise textures. While this certainly leads to a more easily "readable" representation of the object, it is of course impossible to recover object information that is lost due to a lack of signal strength. Further, if the noise level becomes too high, fine-structured information of the object will be removed as the TV constraint cannot distinguish between actual object features and noise patterns. A critical issue, therefore, is how much weight should be put on the TV minimization. If chosen too high, object details will be removed; if too low, the image remains noisy. For the reconstructions presented here the weight was adapted manually to yield images with a comparable noise level as judged by visual inspection. A more routine use of the proposed method would need an automatic mechanism to find an appropriate weight. This, however, requires a reliable noise estimator for the data, which is a nontrivial problem and outside the scope of the current work.

Another open question arises from artifacts caused by spatially varying T1 relaxation during long-stimulated echo trains. In Cartesian sampling the affected point-spread function along the phase-encoding dimension of the image leads to localized one-dimensional blurring. For radial encodings, the image resolution remains mostly unaffected, but instead smearing or streaking artifacts might appear in the object (bottom right image of Fig. 6). Unfortunately, such artifacts are sometimes hardly distinguishable from actual object features, and because the T1 relaxation time is a locally varying quantity, it is basically impossible to fully compensate for the artifacts using a global approach. In practical terms, it might be best to avoid such problems by not using too many echoes in a train—a desirable feature anyhow as it reduces the measuring time by exploiting the radial undersampling properties. On the other hand, a time-segmented reconstruction approach might deal with the problem but would require a priori knowledge or estimation of a relaxation map in order to calculate snapshots of the object according to the T1 weighting of each spoke. Possibly, this information could be extracted directly from the same data using individual reconstructions from each segment of an interleaved reordering scheme.

CONCLUSIONS

This work presents a new method for high-speed MRI based on the use of radial encoding for single-shot STEAM imaging. This combination adds complementary advantages: on the one hand, the RF refocused stimulated echoes allow for the unrestricted utilization of radial *k*-space sampling which for gradient echoes would be hardly possible due to the pronounced off-resonance sensitivity. On the other hand, the undersampling capability of the radial encoding scheme makes optimal use of the limited magnetization available in single-shot STEAM MRI. Because the base resolution can be selected independently from the number of stimulated echoes, the proposed method offers a much higher in-plane resolution than achievable using comparable Fourier encoded versions.

REFERENCES

1. Frahm J, Haase A, Matthaei D, Merboldt K, Hänicke W. Rapid NMR imaging using stmiulated echoes. J Magn Reson 1985;65:130–135.
2. Nolte UG, Finsterbusch J, Frahm, J. Rapid isotropic diffusion mapping without susceptibility artifacts. Whole brain studies using diffusion-weighted single-shot STEAM MR imaging. Magn Reson Med 2000;44:731–736.
3. Rieseberg S, Merboldt KD, Küntzel M, Frahm J. Diffusion tensor imaging using partial Fourier STEAM MRI with projection onto convex subsets reconstruction. Magn Reson Med 2005;54:486–490.
4. Trouard TP, Sabharwal Y, Altbach MI, Gmitro AF. Analysis and comparison of motion-correction techniques in diffusion-weighted imaging. J Magn Reson 1996;6:925–935.
5. Block KT, Uecker M, Frahm J. Undersampled radial MRI with multiple coils. Iterative image reconstruction using a total variation constraint. Magn Reson Med. 2007;57:1086–1098.
6. Frahm J, Merboldt KD, Hänicke W, Haase A. Stimulated echo imaging. J Magn Reson 1985;64:81–93.
7. Speier P, Trautwein F. Robust radial imaging with predetermined isotropic gradient delay correction. Proc Intl Soc Magn Reson Med 2006;14:2379.
8. Karaus A. Weiterentwicklung der schnellen Magnetresonanz-Tomografie mit stimulierten Echos. Diplomarbeit, Universität Tübingen, 2007.